ARCHIVES OF ELECTRICAL ENGINEERING VOL. 59(1-2), 79-86 (2010)

DOI 10.2478/s10171-010-0006-z

Squirrel cage induction motors with idle bars

JAKUB BERNATT

Research & Development Centre of Eletrical Machines KOMEL
188 Rożdzieńskiego, 40-203 Katowice, Poland
tel. +48 32 258 20 41, fax: +48 32 259 99 48
e-mail: jakub.bernatt@komel.katowice.pl

(Recived: 18.11.2009, revised: 14.12.2009)

Abstract: The paper describes high output induction motors driving large applications of heavy starting conditions. Heavy start is characterised by long accelerating time and occures in drives of hudge inertia torque, esspecially when performed at full load. The reliable operation of the motors depends on proper design and quality of rotor's cage. The aspects of thermal behaviour and electrodynamic forces have to be considered during the design of the motor for hard working conditions. In the paper the rotor with idle bars is investigated.

Key words: induction motor, squirrel cage, idle bar, hard working conditions

1. Identification of rotor cage damage causes

Biggest mechanical an thermal stresses occure in rotor cage at starting time of the motor. They result from starting current of big intesity, having its electrodymamic and thermic consequences. They can cause fractures or even melting of the rotor cage. Figure 1 shows the standard course of motor's starting current.

Starting current in rotor bars induces electrodynamic force in its own magnetic field, and this force in turn generates mechanical stress in squirrel cage. If neglected the reactive component of starting current, then bar's current i_p flowing during start-up is identical in form to stator current i_1, and its value is multiplied by electrical voltage ratio [2]

$$i_p \approx i_1 \frac{2m_1 z_1 \zeta_1}{\dot{Z}_2} . \tag{1}$$

The electrodynamic force acting upon a rectangular bar of l length and b width is defined as:

$$F(t) = lb \int_0^h B(y,t) j(y,t) dy . \tag{2}$$

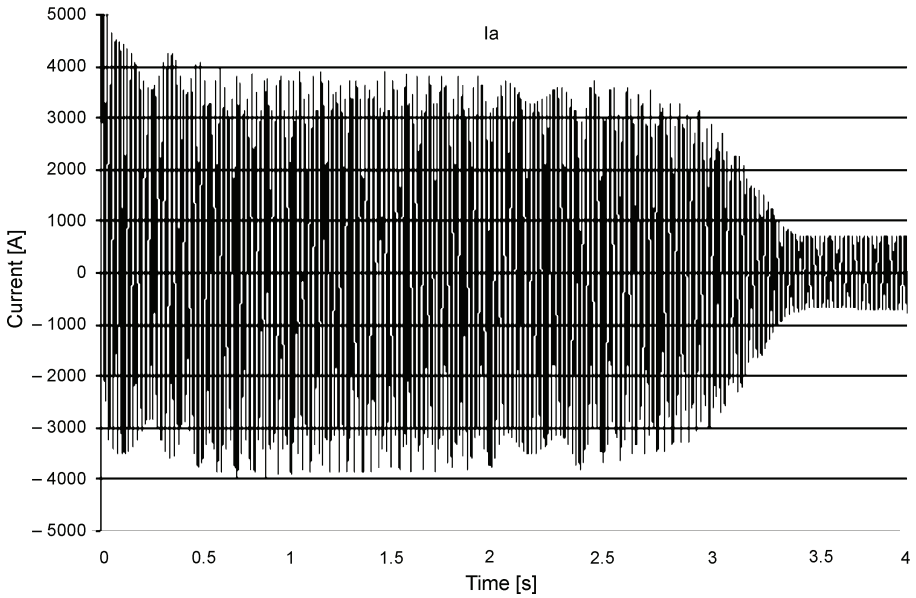

Fig. 1. Motor's starting current at correct start-up

Figure 3 shows distribution of magnetic flux density $B(y, t_1)$ and distribution of current density $j(y, t_1)$ in deep bar at the beginning of start-up ($t = t_1$). When magnetic flux and current density distributions equations ($B(y, t)$ and $j(y, t)$) are identified and integrated, the following relationship is obtained:

$$F(t) = \mu_0 l \frac{I_{p_m}^2}{4b}(1 - \cos 2\omega_2 t) \,. \tag{3}$$

The force $F(t)$ is variable, its vector points down the bar and its frequency is equal to $2f_2$ (f_2 – rotor's current frequency). If the bars have adequate clearance in the slots, then $F(t)$ force generates bar vibrations. Each of the bars is a vibrating beam with its extremities fixed to cage end-ring. These vibration cause fatigue cracking of the bars, mostly close to the rings. The motors which undergo frequent start-ups are prone to cage damages.

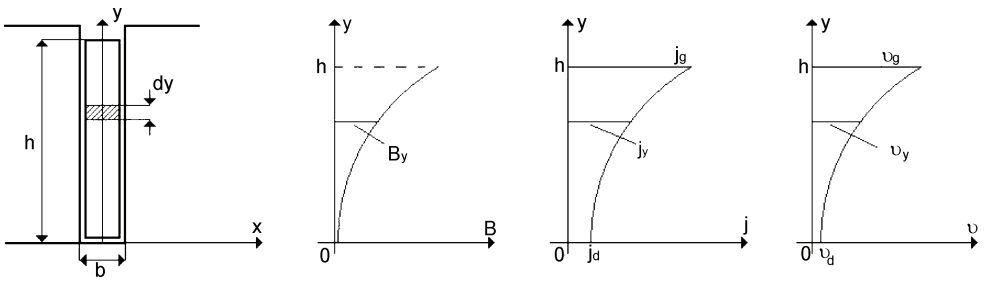

Fig. 2. Deep bar: distribution of magnetic flux densit B_y, current density j_y at the beginning of start-up and temperature distribution in the final stages of the start

The other cage destructive force is of thermal nature. The current density in the bars is non-uniform (see Fig. 2), the current is displaced outwards, towards the magnetic gap. The power losses $d\Delta P_{\mathrm{Cu}}$ in the bar layer dy at the height y are equal to:

$$d\Delta P_{\mathrm{Cu}}(y,t) = \frac{lb}{\gamma_{\mathrm{Cu}}} j^2(y,t)dy \,, \tag{4}$$

where

$$b\int_0^h j(y,t)dy = i_p(t) \,.$$

The instantaneous power distribution $\Delta P_{\mathrm{Cu}}(y, t)$ in the bar is proportional to the power of current density $j^2_{\mathrm{Cu}}(y,t)$, which determines bar temperature distribution $\vartheta(y, t)$ during start-up – Fig. 3.

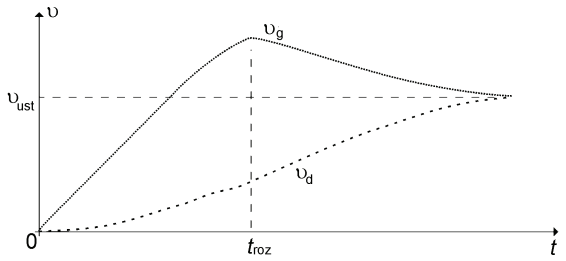

Fig. 3. Temperature course at bar bottom ϑ_d and bar top ϑ_g in the period of motor's start

Temperature distribution $\vartheta(y, t)$ in the bar during start-up is affected, secondarily, by the heat flow along the y coordinate and heat transfer to the rotor iron. The non-uniform temperature distribution generates thermal stress in the bar. This stress is one of the causes of fatigue defects of the rotor cage, it is in particular true for motors with long start-up time [3, 4]. Similar phenomena occur in rotor cages with different slot shapes, including double-cage rotor windings. In double-cage rotors the starting current is mostly appropriated to the upper (starting) cage and this cage usually gets damaged.

Apart from reasons for cage damage stated above, there are lots of other effects accelerating rotor cage wear. Primarily, these are slot clearance, centrifugal forces, rotor unbalance, loose mounting of end-rings, static stresses in places where bars are soldered to the end-rings.

2. Rotor with "idle" bars

Searching for rotor cage design with minimised mechanical stresses due to electromagnetic and thermal causes has resulted in so-called starting bars ("idle bars") cage design [1, 5]. Such motors have been manufactured for many years in US [1]; in Europe at first by ASEA com-

pany (now ABB). These were 4, 6 and 8-pole motors with rated power ranging from 800 kW to 22 MW. The starting (idle) bars located in upper part of rotor slots are not connected by the end-ring and they may undergo deformation freely, the occurring stresses in the bars are low and do not cause any damage to the winding. The "idle" bar is not subjected to slot electrodynamic forces. Fig. 4 shows rotor winding with squirrel cage ("active" bars) and idle ("start-up") bars. The active bars are short-circuited at the ends by the end-rings.

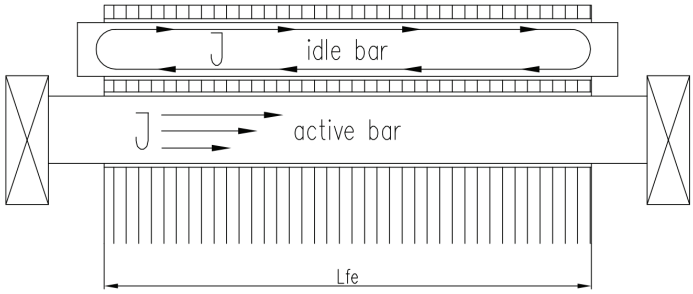

Fig. 4. Rotor containing "idle" bars

Voltage is induced in rotor bars by principal magnetic flux; this voltage in turn causes flow of current in "active" bars. The "idle" bars lie within the range of slot leakage magnetic field of "active" bars, this induces flow of current in "idle" bar (Fig. 4, 5).

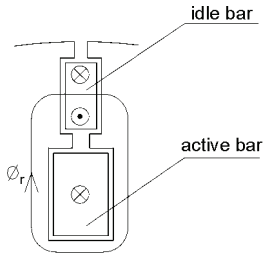

Fig. 5. Currents and slot leakage flux in "idle" bar rotor

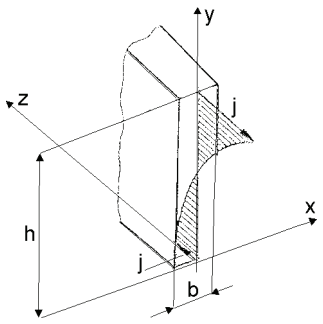

Fig. 6. Current density distribution in the "idle" bar at the beginning of start-up ($s = 1$)

Current density in "idle" bars is distributed along its height as shown at Fig. 6. At the rated (nominal) speed the current in "idle" is low and their influence on electromechanical characteristics is negligible. The total current in "idle" bar is equal to

$$i_b = b\int_0^h j dy = 0 \tag{5}$$

and therefore electrodynamic force acting upon the bar is nil. In motors with "idle" bars, the active bars during start-up exhibit lower temperature gradient than deep bars. Theory of induction motors states that during start-up the heat energy released in rotor circuit is equal to the sum of mechanical energy gained in the rotor and energy transmitted via the shaft to the driven machines. In "idle" bar motor the greater part of this energy is released in the "idle" bars, so that they heat up faster and reach higher temperatures than "active" bars. "Idle" bar current density distribution shows (Fig. 6) that these bars do not become heated uniformly, since most of the heat is released in bars outer layers. Hence thermal stresses are much lower than deep bar stresses, they are usually compensated along the bar height and may cause insignificant deformations only. Apart from this fact, the "idle" bars are free (not fixed to the end-ring) and may be deformed without any adverse effect on cage durability.

If slot dimensions of "idle" bars motors are optimised, start-up torque, maximum torque and start-up current values obtained are comparable with corresponding double-cage motor values [7]. Eliminating electrodynamic stresses and limiting thermal stresses makes it possible to increase start-up load. In case of drive using "idle" bars induction motors it is possible to allow start-up time *c*. 50% longer than in deep bar motors and 2-3 times longer than in double-cage motors; it is also allowable to repeat start-ups one directly after another.

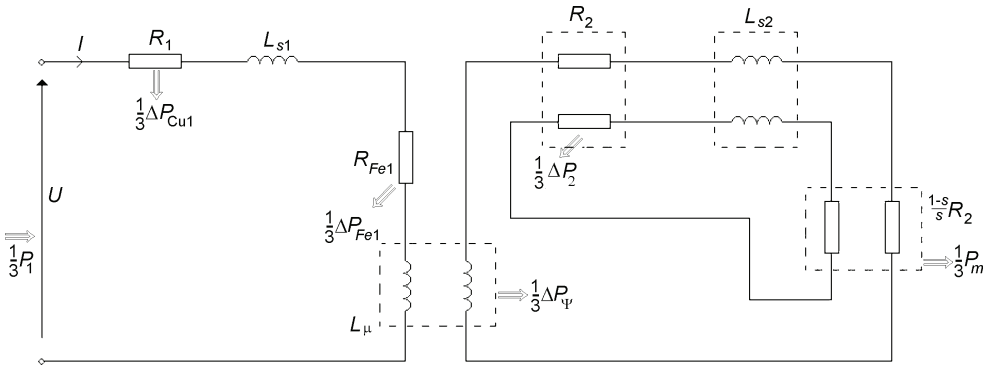

Fig. 7. Equivalent scheme of induction motor with "idle" rotor bars

The equivalent scheme of "idle" bar motor may be constructed as a two-terminal network shown in Fig. 7. The power balance may be expressed as:

$$P_1 = \Delta P_{\mathrm{Cu1}} + \Delta P_{\mathrm{Fe1}} + P_{\Psi}\ , \tag{6}$$

$$P_{\psi} = \Delta P_2 + P_m \ . \tag{7}$$

Loss energy

$$\int_0^{t_r} [\Delta P_{\mathrm{Cu1}} + \Delta P_{\mathrm{Fe1}} + \Delta P_2]dt \tag{8}$$

is dissipated inside the motor in the form of heat; in particular this energy

$$\int_0^{t_r} \Delta P_2 dt = \frac{1-s}{s} \int_0^{t_r} P_m dt \tag{9}$$

is dissipated in the rotor (in operational cage, in "idle" bars and in rotor iron). The course of power transmitted via the air gap during motor start-up determines motor's electromagnetic torque. If the start-up time is long enough, than the real current and torque time courses may be approximated with quasi-steady waveforms. The electromagnetic torque vs. slip may then be expressed as:

$$T_{em}(s) = \frac{P_m(s)}{\omega_m(s)} = \frac{P_{\psi}(s)p}{\omega_1} \ , \tag{10}$$

where: $\omega_m(s)$ is rotor's rotational speed, and ω_1 is the rotating field angular speed.

3. Design example

The SZJr 138r motors rated at 400 kW, 6 kV, 740 rpm are used to drive coal mills and melting mills in one of the steel plants. The original make of the motor has trapezoidal deep rotor bars, fastened by steel wedges at the slot bottom (see drawing in Table 1). These drives may exhibit start-up times as long as 30 seconds (if, for example, the mill is full), while the original make motor's allowable star-up time is defined as 20 seconds. High failure rate of these motors has led to modernisation of cage winding design. It has been decided to apply cage winding utilising "idle" bars, with slot and bar shape as shown in Table 1. Slot clearances have been eliminated by rolling the outer surface of "idle" bars. The following data are given in Table 1: rotor slot and bar shapes, number of turns of stator winding z_1 , results of calculations of basic motor parameters. Figure 7 shows torque vs. slip characteristics. From the calculations it may be concluded that if stator winding data is not changed, then overload capacity of motor with "idle" bars is less than in case of motor with trapezoidal bars; however, the start-up torque is greater. Torque overload capacity may be increased by reducing stator winding's number of turns, i.e. by increasing magnetic flux. The "idle" bar motor efficiency is lower than original motor's efficiency by 0.6%. This design has passed practical tests, the "idle" bar motors are able to withstand start-up time of up to 40 seconds and their durability is several times higher comparing to standard motors with deep bar rotors.

Table 1. Motor data

No.	Motor variant		1	2a	2b
1	Slot and rotor bars shape and dimensions		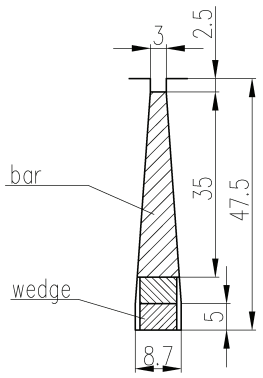	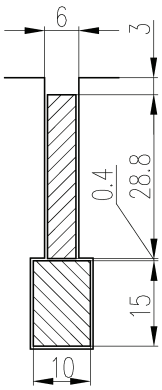	
2	Z_1		336	336	312
3	P_{1N}	kW	400	400	400
4	U_N	kV	6	6	6
6	I_N	A	49.8	52	52.5
7	T_N	$N{\cdot}m$	5 160	5 160	5 160
8	cosφ	–	0.84	0.81	0.80
10	s_N	%	1.4	1.8	1.5
11	η	%	91.9	91.2	91.4
12	I_r/I_N	–	4.6	3.9	4.5
13	T_r/T_N	–	1.1	1.4	1.6
14	T_m/T_N	–	2.1	1.8	2.0
15*	$\Delta\vartheta_{z1}/t_r$ $\Delta\vartheta_{kg}/t_r$ $\Delta\vartheta_{pier}/t_r$ $\Delta\vartheta_{pb}/t_r$	deg/s	1.8 3.9 1.9 –	1.4 4.7 2.3 16.4	1.7 4.8 2.4 19.3

*) – rate of temperature increase in the first second of the starting: $\Delta\vartheta_{z1}/t_r$ – in upper part of the tooth, $\Delta\vartheta_{kg}/t_r$ – in upper (operational) cage surface, $\Delta\vartheta_{pier}/t_r$ – in the end-rings and $\Delta\vartheta_{pb}/t_r$ – in upper part of "idle" bars

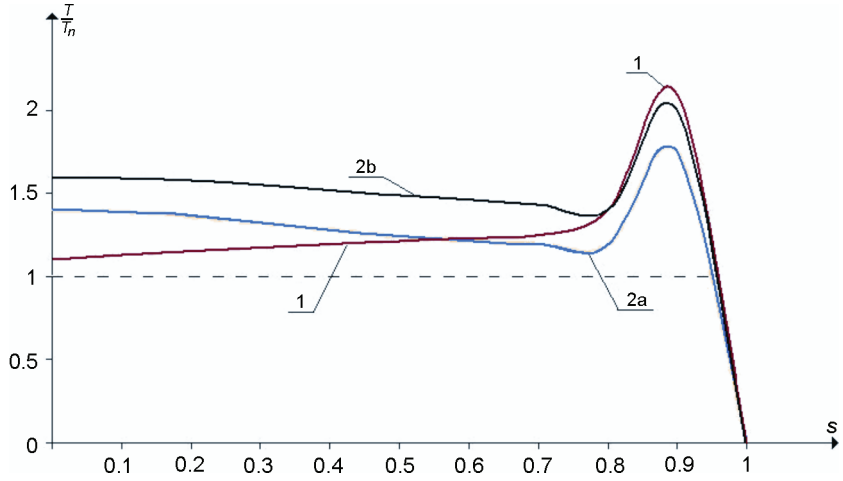

Fig. 7. Electromagnetic torque vs. motor slip-motors as per Table 1

References

[1] P. Alger, *Induction machines, their behavior and uses*.Gordon an Breach, N. York 1970.

[2] W. Schuisky, *Berechnung elektrischer Maschinen*. Springer Verlag, Wien 1957.

[3] B. Śliwa, *Własności rozruchowe silników klatkowych z prętami biernymi w wirniku*. (*Starting performance of induction motors with idle bars in the rotor*) Przegląd Elektrotechniczny 5: 204-207 (1979).

[4] M. Bernatt, J. Mróz, R. Rut, *Zakłócenia rozruchu silnika indukcyjnego klatkowego wskutek niedomagań łącznika sieciowego*. (*Starting disturbances of an induction motor caused by the switch troubles*) Zeszyty Problemowe – Maszyny Elektryczne Komel 65: 139-141 (2003).

[5] W. Schuisky, *Kafigwicklungen der Asynchronmotoren*. Materiały na Krajową Konferencję Napędu Elektrycznego i Energoelektroniki, AGH: 29, Kraków 1977.

[6] G. Leroy, R. Chavernoz, M. Simon *L'experimentation entreprise au Banc d'Essai de l'Electricite de France dans le domaine des rotors a cage*. (*Results of tests of squirrel cage rotors at EdF test station*) RGE 9, 1047 (1966).

[7] B. Śliwa, M. Bernadt *Silniki indukcyjne z prętami biernymi – nowe rozwiązanie silnika klatkowego*. (*Induction motors with idle bars in the rotor*) Zeszyty Problemowe – Maszyny Elektryczne Komel 31: 14-22 (1980).